International Journal of Digital Information and Wireless Communications (IJDIWC) 1(1): 195-203
The Society of Digital Information and Wireless Communications, 2011 (ISSN 2225-658X)

Intelligent Bubble Recognition on Cardiac Videos using Gabor Wavelet

Ismail Burak PARLAK[1,2,*], Salih Murat EGI[1,5], Ahmet ADEMOGLU[2], Costantino BALESTRA[3,5], Peter GERMONPRE[4,5] and Alessandro MARRONI[5]

[1]Galatasaray University, Department of Computer Engineering, Istanbul, TURKEY
[2]Bogazici University, Institute of Biomedical Engineering, Istanbul, TURKEY
[3]Environmental & Occupational Physiology Laboratory Haute Ecole Paul Henri Spaak, Brussels, BELGIUM
[4]Centre for Hyperbaric Oxygen Therapy, Military Hospital, B-1120 Brussels, BELGIUM
[5]DAN Europe Research Division, BELGIUM

Mailing Address: Ciragan Cad. No:36, Ortakoy 34357, Istanbul
E-mail:bparlak@gsu.edu.tr

ABSTRACT

In cardiology, automatic recognition and image analysis still conserve computational challenges in terms of medical guidance and diagnosis. Bubbles or microemboli that circulate into cardiopulmonary system are considered suspicious for several medical problems such as decompression sickness, stroke and migraine. The aim of our work is to develop and assess an automatic approach to detect these bubbles that are analyzed manually by clinicians. In this paper, five different divers were examined in post decompression phase and their cardiac videos were recorded. Existent bubbles on the frames were also marked by two specialists in order to compare with our results. We developed our neural network architecture by integrating Gabor-Wavelet kernel which is commonly used in face and pedestrian recognition. The training phase of the network was performed using real bubble morphologies. Our recognition phase was achieved on four cardiac chambers through echocardiographic frames. Our correct detection ratio was between 77.6-94.3%. We consider that our approach would be useful in longitudinal researches in hypobaric and hyperbaric environments and risky subjects with congenital defects.

KEYWORDS

Echocardiography, Artificial Neural Networks, Venous Emboli, Decompression Sickness.

1 INTRODUCTION

Over the last decades, decompression sickness which is a severe problem in both professional and recreational diving was treated by multidisciplinary research groups. Medical and computational studies revealed new approaches to prevent unwanted effects and to reduce injuries during post decompression phase. Initial applications were diving tables and timing algorithms in this field. Even if related procedures decreased diving pitfalls, a compact system has not yet developed in order to resolve relevant medical problems due to the complexity of inter physiological systems and computational restrictions.

Most of the decompression illnesses (DCI) and side effects are classified as unexplained cases though all precautions were taken into account. As a matter of fact, mathematical models and simulations focused on the effects of micro emboli in circulation and cardiopulmonary system. Balestra et al. [1] emphasized bubble physiology and morphology in the prevention of DCI and strokes.

Furthermore, Blatteau et al. [2] reviewed how these micro structures would form within musculoskeletal activities and their pathways. It is also remarkable that physical activities in hyperbaric environments would cause big variations in bubble creation between different subjects and even for same subjects in different dives.

As first computational analysis in this field, bubble patterns were recognized and classified in sound forms using Doppler ultrasound in different studies [3, 4]. Doppler modality is preferred for post decompression in terms of portability and quick diagnosis. However these sound records are limited to venous examinations and all existent bubbles in circulation would not be observed. The interference of speckle noise, the lack of shape and motion information related to emboli morphology and variations in diagnosis between clinicians are other pitfalls of this modality.

2D Echocardiography which is available nowadays in portable forms serves as better modality in this area and bubble recognition. Clinicians generally count bubbles manually within this modality and this human eye based recognition would cause big variations between trained and untrained observers [5]. Initial procedures to automatize this detection are based to either fixed region of interests (ROI) [6,7] or variation of pixel intensities [8]. It is obvious that objective recognition in echocardiography is always a difficult task due to image quality. Image quality is always correlated with probe and patient stabilization, the experience of clinicians, acquisition setup and device specifications. Inherent speckle noise and temporal loss of view in apical four chambers are major problems through computerized analysis.

In general, bubble detection would be modeled in two different ways. Firstly, bubbles would be detected in a human based optimal ROI (left atrium, pulmonary artery, aorta) which is specifically known in the heart. This procedure would require a segmentation process. However, all existent bubbles would not be detected and this would limit an accurate assessment of bubble activities. Secondly, bubbles would be detected in whole cardiac chambers and they might be counted without a preprocessing step. This approach would benefit the temporal evaluation of long lasting records and complete bubble number.

In this paper, we aimed an automatic bubble recognition using Artificial Neural Networks (ANN) without segmenting cardiac chambers. High rate of object recognition proved the utility of ANN in several fields. On the other hand, their adaptive structure would be reduced when training phase and their initial setup are not correctly carried out.

Therefore, false positives would interfere and mislead satisfactory object recognition. For this purpose, a good training phase and reasonable network architecture become crucial to provide detection results in acceptable range. Gabor wavelet is a method to detect, filter or reconstruct variant object forms. It is integrated with ANN for different applications such as face, pedestrian recognition and biometrics [9-14] and it is preferred as an imitator of human wise recognition.

In our study, we hypothesize that automatic bubble recognition would reveal an accurate assessment and optimize the subjectivity between clinicians on cardiac videos. Post decompression records in echocardiography are considered to survey unexplained decompression illness which is commonly examined by standardized methods such as dive computers and tables. Moreover, detected bubbles over atria would be a potential risk for probable hypoxemia, stroke and migraine. Even if image quality, Transthoracic Echocardiography (TTE) modality and acquisition protocol would be limitation factors for detection rates, we conclude that our findings would offer a better interpretation of existent bubbles.

2 METHODS

This study was performed on five male professional divers. Each subject provided written informed consent before participating to join the study. Video recording and archiving were carried out using Transthoracic Echocardiography (3-8 Mhz, MicroMaxx, SonoSite Inc, WA) which is a non invasive and over cutaneous imaging modality. For each subject, three different records between 2.8--3.2 minutes were digitally stored in high resolution avi format. Videos are recorded with 25 frames per second (fps) and 640x480 pixels as resolution size. Therefore, for each patient 4000-4500 frames were taken into account. All records were evaluated double blinded by two trained clinicians on bubble detection.

In this study, Gabor kernel which is generalized by Daugman [15] was utilized to perform the Gabor Wavelet transformation. Gabor Transform is preferred in human wise recognition systems. Thus, we followed a similar reasoning for the bubbles in cardiology which are mainly detected depending on the visual perception of clinician.

$$\Psi_i(\vec{x}) = \frac{\left\|\vec{k}_i\right\|^2}{\sigma^2} e^{-\frac{\left\|\vec{k}_i\right\|^2 \|\vec{x}\|^2}{2\sigma^2}} \left[e^{j\vec{k}_i\vec{x}} - e^{-\frac{\sigma^2}{2}} \right] \quad (1)$$

Here each $\boldsymbol{\Psi i}$ surface is identified with $\boldsymbol{k_i}$ vector. $\boldsymbol{k_i}$ vector is engendered through Gauss function with standard deviation $\boldsymbol{\sigma}$. The central frequency of *i*th filter is defined as;

$$\vec{k}_i = \begin{pmatrix} k_{ix} \\ k_{iy} \end{pmatrix} = \begin{pmatrix} k_v cos\theta_\mu \\ k_v sin\theta_\mu \end{pmatrix} \quad (2)$$

where;

$$k_v = 2^{\frac{-v+2}{2}} \qquad v \in \{0,..,4\} \quad (3)$$

$$\theta_\mu = \mu\frac{\pi}{8} \qquad \mu \in \{0,..,7\} \quad (4)$$

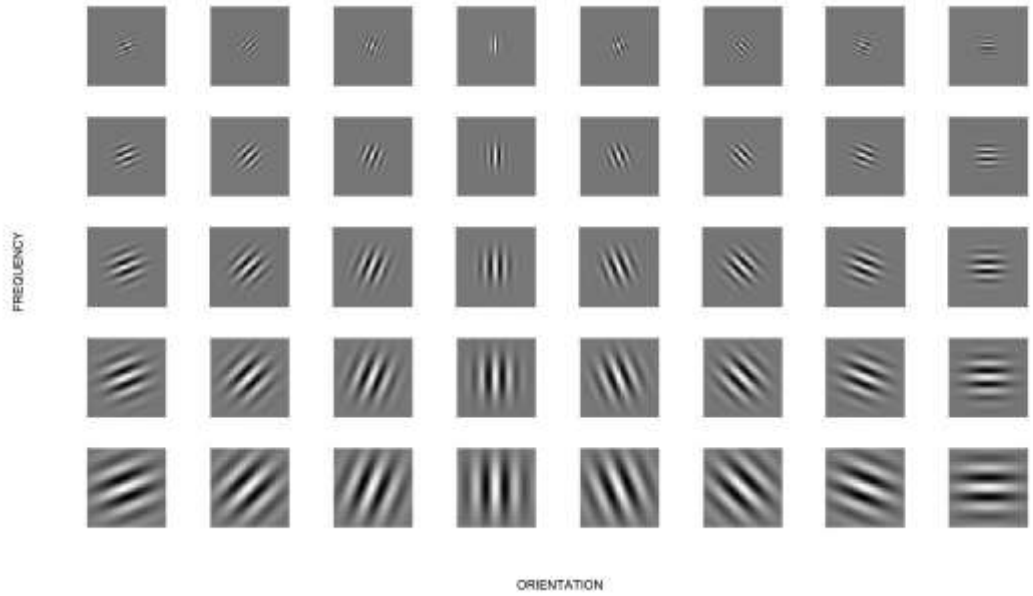

The $\boldsymbol{v}$ and $\boldsymbol{\mu}$ express have spatial frequency and eight orientations, respectively. These structures are represented in Figure 1.

Figure 1. Gabor wavelet for bubble detection

weight vectors are defined using Nguyen Widrow method.

Hyperbolic tangent function is utilized as transfer function during learning phase. This function is defined as it follows;

$$tanh(x) = \frac{e^{2x} - 1}{e^{2x} + 1} \qquad (5)$$

ANN architecture was constructed as feed forward neural network which has three main layers. While hidden layer has 100 neurons, output layer has one output neuron as in Figure 2. The initial

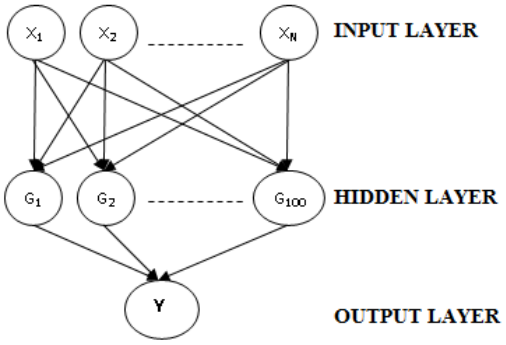

Figure 2. Block Diagram of feed forward ANN.

Our network layer was trained with candidate bubbles whose contrast, shape and resolution are similar to archived videos. 250 different candidate bubble examples were manually segmented

from different videos apart from TTE records in this paper. Some examples from these bubbles are represented in Figure 3.

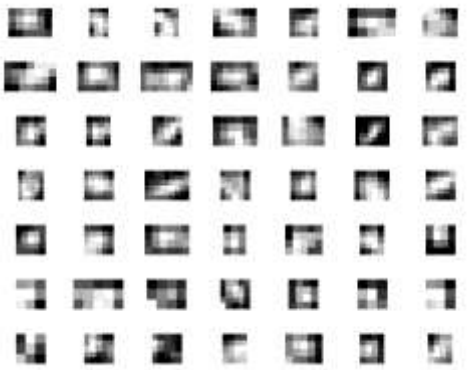

Figure 3. Examples of training bubbles.

All TTE frames within this study which may contain microemboli were firstly convolved with Gabor kernel function. Secondly, convolved patterns were transfered to ANN. Output layer expressed probable bubbles onto the result frame and gave their corresponding centroids.

After the detection we performed a statistical analysis to observe Type 1 and 2 errors and to reveal the sensitivity and specificity of our proposed approach.

3 RESULTS

In all subjects who were staying in post decompression interval, we found microemboli in four cardiac chambers. These detected bubbles in all frames were counted for each subject and compared with human wise detection. The accuracy of our findings and detection errors are given in Table 1 and 2.

In our initial phase of detection, we had the assumption of variant bubble morphologies for ANN training phase in Figure 3. As it might be observed in Figure 4, detected nine bubbles are are located in different cardiac chambers. Their shapes and
surfaces are not same but resemble to our assumption.

Even if all nine bubbles in Figure 4 would be treated as true positives, manual double blind detection results revealed that bubbles 5, 8 and 9 are false positives. We observe that our approach would recognize probable bubble spots through our training phase but it may not identify nor distinguish if a detected spot is a real bubble or not.

In this case of Figure 4 it might be remarked that false positives are located on endocardial boundary and valves. These structures are generally continuously visualized without fragmentation. However patient and/or probe movements may introduce convexities and discontinuities onto these tissues which will be detected as bubbles.

We performed a comparison between double blind manual detection and ANN based detection in Table 1. Our bubble detection rates are between 77.6-94.3%.

We observe that bubbles are mostly located in right side of heart which is a physiological effect. Bubbles in circulation would be filtered in lungs. Therefore fewer bubbles are detected in left atria and ventricle.

In order to evaluate the correctness of detection and the accuracy of bubble distribution, all records were analyzed double blinded. In Table 1, we note that detection rates may differ due to visual speculation of human bubble detection in boundary zones, artifacts or within suboptimal frames. In Table 2, the evaluation of Type 1 and 2 errors give the sensitivity (90-95%) and specificity (64-73%) of computational detection.

4 DISCUSSION&CONCLUSION

Post decompression period after diving consist the most risky interval for probable incidence of decompression sicknesses and other related diseases. Hyperbaric environments which trigger the formation of free nitrogen bubbles might circulate through cardiopulmonary system and cause severe problems. Cardiac imaging is the golden standard as a medical routine to survey bubble pathways and diagnosis. It is remarkable that cardiac video imaging is the fundamental step to prevent injuries and cerebral imaging is utilized when diseases occur. Therefore, more studies in bubbles are oriented into circulation problems through cardiopulmonary system.

Microemboli which are the main cause of these diseases still conserve medical and computational challenges for objective assessment. However, their chaotic behavior into circulation system and their physical properties reduce objective monitoring and cause interrater variations in terms of counting and morphology.

Nowadays, mathematical models and computational methods developed by different research groups propose a standardization in medical surveys of decompression based evaluations. Actual observations in venous gas emboli would reveal the effects of decompression stress. Nevertheless, the principal causes under bubble formations and their incorporations into circulation paths are not discovered. Newer theories which maintain the principles built on Doppler studies, M-Mode Echocardiograhy and Imaging propose further observations based on the relationship between arterial-endothelial tissues and bubble formations. On the other hand, there is still the lack and fundamental need of quantitative analysis on bubbles in a computational manner.

For this purposes, we applied a full automatic procedure to resolve the main problem bubble studies. We detected synchronously microemboli in whole heart by mapping them spatially through their centroids. It is clear that our method would offer a better perspective for both recreational and professional dives by the means of accurate detection rates (Table 1) and high sensitivity and specificity (Table 2).

On the other hand, we note that detection methods might suffer from blurry video records. Even if apical view of TTE offered the advantage of complete four chambers' view, we were limited to see some chambers with a partial aspect due to patient or probe movement during recording phase. Therefore, image quality and clinician experience are fundamental requirements for good performance in automatic analysis.

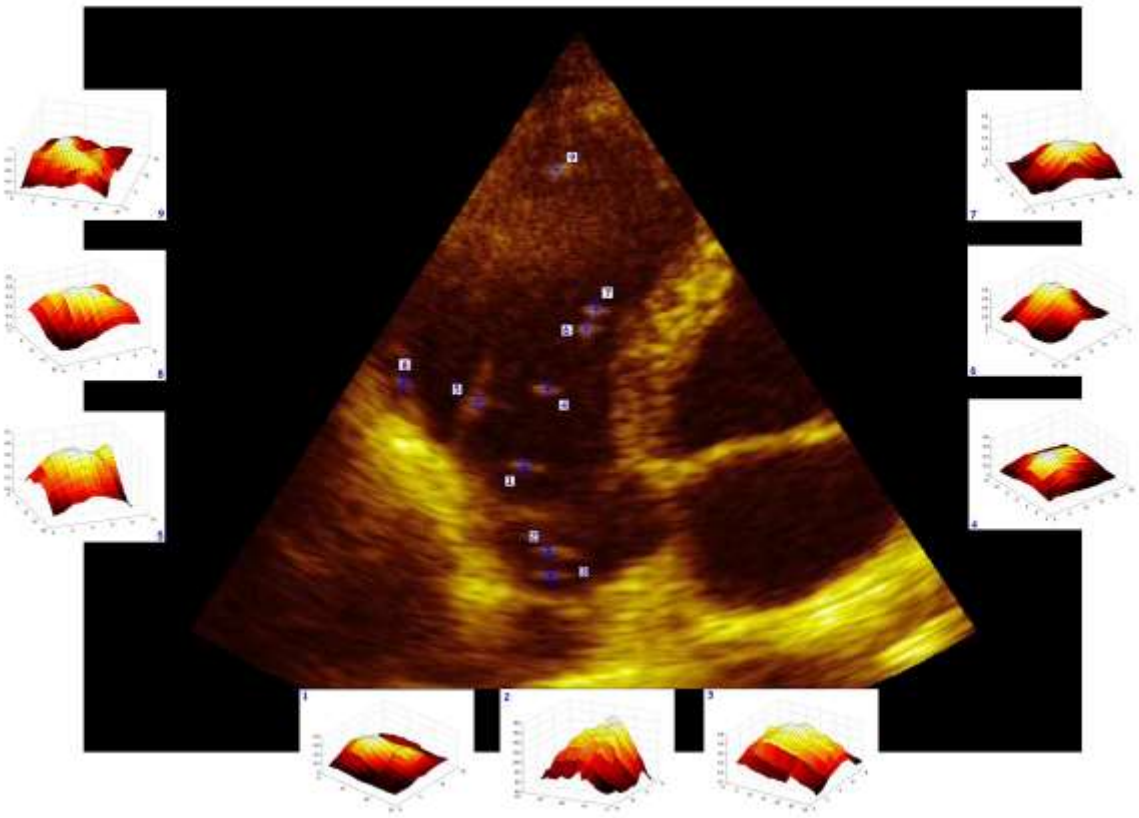

Moreover, resolution, contrast, bubble brightness, fps rates are major factors in ANN training phase. These factors would affect detection rates. When resolution size, whole frame contrast differ it is obvious that bubble shape and morphologies would be altered.

It is also remarkable to note that bubble shapes are commonly modeled as ellipsoids but in different acquisitions where inherent noise or resolutions are main limitations, they would be modeled as lozenges or star shapes as well.

In this study, ANN training is performed by candidate bubbles with different morphologies in Figure 3. In the prospective analysis, we would train our network hierarchy through non candidate bubbles to improve accuracy rates of detection. As it might be observed in Figure 4 false positive bubbles intervene within boundaries. These regions consist of endocardial boundary, valves and blurry spots towards the outside extremities. We conclude that these non

Figure 4. Centroids of detected bubbles and their spatial representations

bubble structures which lower our accuracy in detection and classification might be eliminated with this secondary training step.

6 REFERENCES

1. Balestra, C., Germonpre, P., Marroni, A., Cronje, F.J.: PFO & The Diver. Best Publishing Company, Flagstaff (2007)
2. Blatteau, J.E., Souraud J.B., Gempp, E., Boussuges A.: Gas nuclei, their origin, and their role in bubble formation. Aviat Space Environ Med. 77, 1068--1076 (2006)
3. Tufan K., Ademoglu A., Kurtaran E., Yildiz G., Aydin S., Egi S.M.: Automatic detection of bubbles in the subclavian vein using Doppler ultrasound signals. Aviat Space Environ Med. 77, 957--962 (2006)
4. Nakamura H., Inoue Y., Kudo T., Kurihara N., Sugano N., Iwai T.: Detection of venous emboli using Doppler Ultrasound. European Journal of Vascular & Endovascular Surgery. 35, 96--101 (2008)
5. Eftedal O., Brubakk A.O.: Agreement between trained and untrained observers in grading intravascular bubble signals in ultrasonic images. Undersea Hyperb Med. 24, 293--299 (1997)
6. Eftedal O., Brubakk A.O.: Detecting intravascular gas bubbles in ultrasonic images. Med Biol Eng Comput. 31, 627--633 (1993)
7. Eftedal, O., Mohammadi, R., Rouhani, M., Torp, H., Brubakk, A.O.: Computer real time detection of intravascular bubbles. In: Proceedings of the 20th Annual Meeting of EUBS, pp. 490{494. Istanbul (1994)
8. Norton, M.S., Sims, A.J., Morris, D., Zaglavara, T., Kenny, M.A., Murray, A.: Quantication of echo contrast passage across a patent foramen ovale. In: Computers in Cardiology, pp. 89--92. IEEE Press, Cleveland (1998)
9. Shen, L., Bai, L.:A review on Gabor wavelets for face recognition. Pattern Anal Applic. 9, 273--292 (2006)
10. Hjelmas, E.: Face Detection A Survey. Comput Vis Image Underst. 83, 236--274 (2001)
11. Tian, Y.L., Kanade, T., Cohn, J.F.: Evaluation of Gabor wavelet based facial action unit recognition in image sequences of increasing complexity. In: Fifth IEEE International Conference on Automatic Face and Gesture Recognition, pp. 229--234.
12. Hong, C., Nanning Z., Junjie Q.: Pedestrian detection using sparse Gabor filter and support vector machine. In: Intelligent Vehicles Symposium IEEE, pp. 583--587 (2005)
13. Wai, K.K., David, Z., Wenxin, L.: Palmprint feature extraction using 2-D Gabor filters. Pattern Recognition. 36, 2339--2347 (2003)
14. Yong, Z., Tieniu, T., Yunhong, W.: Biometric personal identification based on iris patterns. In: 15th International Conference On Pattern Recognition pp. 801--804 (2000)
15. Daugman J.G.: Complete discrete 2-D Gabor transforms by neural networks for image analysis and compression. IEEE Trans Acoustics Speech Signal Process. 36, 1169--1179 (1988)

Table 1. Comparison and evaluation of automatic and human wise detection

	Detected Bubbles			Detection Rate of ANN (%)	
	ANN	Clinician 1	Clinician 2	Through Clinician 1	Through Clinician 2
Subject 1	475	405	428	82,72	89,02
Subject 2	1396	1302	1287	92,78	91,53
Subject 3	864	818	800	94,38	92,00
Subject 4	2283	1865	1912	77,59	80,60
Subject 5	2017	1865	1880	91,85	92,71

Table 2. Statistical interpretation of bubble recognition

	True Positives	False Positives	True Negatives	False Negatives	Sensitivity(%)	Specificity (%)
Subject 1	475	83	227	48	90.8	73.2
Subject 2	1396	157	438	64	95.6	73.6
Subject 3	864	163	312	47	94.8	65.7
Subject 4	2283	308	574	122	94.9	65.1
Subject 5	2017	268	489	96	95.5	64.6